THE ASTROPHYSICAL JOURNAL, 207:L53–L55, 1976 July 1

GAS DYNAMICS OF SEMIDETACHED BINARIES. II. THE VERTICAL STRUCTURE OF THE STREAM

STEPHEN H. LUBOW AND FRANK H. SHU
University of California, Berkeley
Received 1975 December 30

ABSTRACT

We consider the three-dimensional dynamics of the stream in semidetached binaries undergoing Roche lobe overflow. We generalize the results of an earlier communication to include the dynamical effects in the direction perpendicular to the orbital plane. We find that the scale height of the stream characteristically exceeds its corresponding hydrostatic value by a significant factor because the inertia of the gas prevents it from responding instantaneously to the changing gravitational field. This effect is important for the interpretation of the observations relating to stream-disk impacts in cataclysmic variables and in binary X-ray sources of low total mass.

Subject headings: stars: binaries — X-rays: sources

I. INTRODUCTION

In an earlier communication (Lubow and Shu 1975, hereinafter referred to as Paper I), we solved the problem of mass transfer in semidetached binaries by the method of matched asymptotic expansions. The small expansion parameter of the problem was the ratio ϵ of the isothermal speed of sound to the relative orbital speed of the two stars. We suppressed the question of the vertical structure of the stream by the simple device of integrating the basic equations over the direction perpendicular to the orbital plane. An estimate for the volume density ρ at stream center was recovered from the computed surface density σ by making the standard assumption of vertical hydrostatic equilibrium (see also Prendergast and Tamm 1974; Flannery 1975).

Because of the large variation of the gravity encountered by the stream, however, we already remarked in Paper I (p. 392) that strict hydrostatic equilibrium in the vertical direction was unlikely to prevail. We have returned to investigate this problem in detail because the vertical extent of the stream relative to the vertical extent of a disk, which may surround the detached component in many systems, can have observable consequences (§ IV). The horizontal aspects of the problem remain identical to that solved in Paper I.

II. THREE-DIMENSIONAL STREAM SPREADING

We use the same notation as Paper I and refer to the equations, tables, and figures of Paper I by the prefix I followed by a decimal point and the corresponding number. To describe the behavior of the stream in the "orbit region" (see Fig. I.1), we adopt the dimensionless "natural coordinates" (s, n, z), where z is the vertical coordinate, s is the distance from the inner Lagrangian point L1 measured along the center of the stream, and n is the third orthonormal coordinate.

The stream is thin in both the n and the z directions; hence, we are motivated to introduce the two length scales: $n_1 = \epsilon^{-1}n$, $z_1 = \epsilon^{-1}z$. The horizontal components of velocity do not vary rapidly with z, whereas the vertical component does not vary rapidly with n. To solve the three-dimensional analogs of equations (I.48), therefore, we try the perturbation series

$$\begin{aligned} \rho &= \epsilon^{-2}\rho_{-2}(s, n_1, z_1) + \dots, \\ u_s &= u_{s0}(s) + \epsilon u_{s1}(s, n_1) + \dots, \\ u_n &= \epsilon u_{n1}(s, n_1) + \dots, \\ u_z &= \epsilon u_{z1}(s, z_1) + \dots, \end{aligned} \tag{1}$$

where the speed of the stream center, $u_{s0}(s)$, is given by ballistic considerations.

To be able to match the right-hand asymptotic behavior in the L1 region (see § III*c* of Paper I), we assume

$$u_{s1} = \alpha(s)n_1, \quad u_{n1} = \beta(s)n_1, \quad u_{z1} = \nu(s)z_1,$$
$$\rho_{-2} = \rho_{-20}(s) \exp\{-\tfrac{1}{2}[\gamma(s)n_1^2 + \chi(s)z_1^2]\}. \tag{2}$$

These forms reduce the perturbational set of partial differential equations to a set of ordinary differential equations which govern the behavior of ρ_{-20}, α, β, γ, ν, and χ as functions of s. The equations which determine α, β, and γ form a closed set; their integration subject to the matching conditions at L1 gives the results tabulated in Table I.3. The equations which determine ν and χ also form a closed set. They read

$$u_{s0}\frac{d\chi}{ds} + 2\nu\chi = 0, \quad u_{s0}\frac{d\nu}{ds} + \nu^2 = -\omega_z^2 + \chi, \tag{3}$$

where $\omega_z^2(s)$, the square of the z-oscillation frequency, is $\partial^2\phi/\partial z^2$ evaluated at the stream center $(s, 0, 0)$. Equations (3) are to be solved under the matching condition that hydrostatic equilibrium prevails in the vertical direction at L1:

$$\nu = 0, \quad \chi = \omega_z^2(0) = A \text{ as } s \to 0, \tag{4}$$

where A is the number defined by equation (I.13). Since the known function $u_{s0}(s)$ vanishes linearly with s at L1, analytic series solutions valid in the neighborhood of $s = 0$ are required to provide correct starting conditions for the numerical integration of equations (3).

The solution is completed by integrating the remaining equation for ρ_{-20}. With the definition that the dimensionless mass transfer rate is unity, we easily obtain

$$\frac{2\pi}{(\gamma\chi)^{1/2}}\,\rho_{-20}u_{s0} = \text{const.} = 1\,. \quad (5)$$

Numerical results are given in Table 1 and Figure 1.

The cases considered in Table 1 correspond to the same cases tabulated in Table I.3. The entries for the scaled volume density at stream center, $\epsilon^2\rho(n = z = 0)$, in Table 1 are less than those in Table I.3 because the true equivalent thickness, $\epsilon(2\pi/\chi)^{1/2}$, is generally larger than the hydrostatic thickness, $\epsilon(2\pi)^{1/2}/\omega_z$. The physical effect can be appreciated as follows.

The vertical gravity increases as the detached component is approached, but the gas in the stream cannot instantaneously adjust to the height appropriate for local hydrostatic equilibrium because the gravity changes too quickly—especially in the middle stages—for the inertia to be neglected. Thus, the true scale height lags behind the hydrostatic value as the stream flows substantially away from L1 (see Fig. 1).

TABLE 1

VERTICAL STRUCTURE OF STREAM

Location	ν	$(2\pi)^{1/2}/\omega_z$	$(2\pi/\chi)^{1/2}$	$\epsilon^2\rho$ (n=z=0)
		$M_D/M_C=0.0667$		
L1...........	0.00	1.01	1.01	...
$\frac{1}{2}s(\varpi_d)$........	−1.83	0.505	0.746	4.08
ϖ_d...........	−34.3	0.082	0.251	8.90
		$M_D/M_C=0.5000$		
L1...........	0.00	0.898	0.898	...
$\frac{1}{2}s(\varpi_d)$........	−1.62	0.487	0.733	2.22
ϖ_d...........	−33.6	0.078	0.275	3.94
		$M_D/M_C=1.6667$		
L1...........	0.00	0.892	0.892	...
$\frac{1}{2}s(\varpi_d)$........	−1.17	0.539	0.807	1.50
ϖ_d...........	−21.6	0.109	0.364	2.16
		$M_D/M_C=4.5000$		
L1...........	0.00	0.934	0.934	...
$\frac{1}{2}s(\varpi_d)$........	−0.715	0.645	0.941	1.08
ϖ_d...........	−11.3	0.182	0.523	1.22
		$M_D/M_C=7.0000$		
L1...........	0.000	0.961	0.961	...
$\frac{1}{2}s(\varpi_d)$........	−0.527	0.711	1.02	0.944
ϖ_d...........	−8.05	0.235	0.621	0.954
		$M_D/M_C=15.0000$		
L1...........	0.000	1.01	1.01	...
$\frac{1}{2}s(\varpi_d)$........	−0.245	0.849	1.18	0.770
ϖ_d...........	−4.38	0.363	0.832	0.638

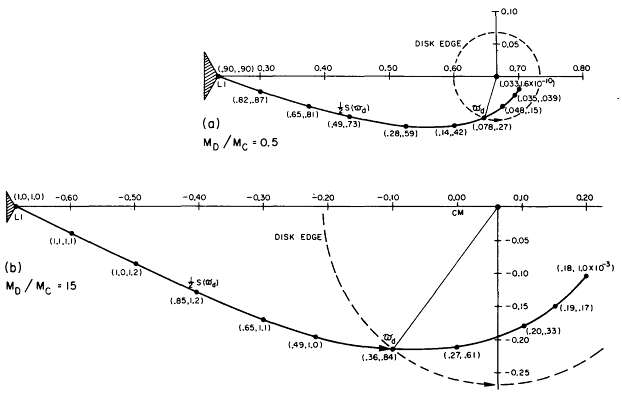

FIG. 1.—Comparison of the scaled hydrostatic and true equivalent thicknesses, $([2\pi]^{1/2}/\omega_z,\ [2\pi/\chi]^{1/2})$. The equatorial plane is viewed face-on for the mass ratios: (*a*) $M_D/M_C = 0.5$, and (*b*) $M_D/M_C = 15$. The origin corresponds to the center of mass, and the orbital separation is unity. Maximum dynamical compression is reached at the rightmost plotted point. This behavior would be interrupted if a dense disk were present with its edge located along the dashed circle. The streamline in the midplane would then be forced by a strong radiating shock to turn parallel to the disk edge as shown schematically by the dashed arrow. The corresponding shock at great distances off the central plane is weak, and very high latitude material in the stream would tend to follow the unperturbed trajectory shown by the solid curve. Intermediate behavior would prevail at intermediate latitudes, and we expect stream material at different heights to be entrained in the disk at different points interior to the disk edge.

The radial velocity of the stream toward the detached component is maximum at approximately the radius, ϖ_d, of the simple periodic orbit which has the same tangential velocity as the stream; and the approach velocity is zero when the stream reaches its minimum distance of approach, $\varpi_{\min}$ (see IV*c* of Paper I). Hence, the discrepancy between the true and hydrostatic scale heights turns out to be largest at about ϖ_d, and the true scale height has a chance to catch and to fall below the hydrostatic value only as the stream nears $\varpi_{\min}$, where the gravity varies slowly.

At about $\varpi_{\min}$, which is located at $\sim 90°$ downstream from ϖ_d, the pressure gradient builds up sufficiently to halt and to reverse the compression. Impact of the stream either with the disk or with the surface of the detached component will generally occur before we have to deal realistically with the phase, near $\varpi_{\min}$, of enormous flattening of the stream toward the orbital plane.

III. IMPACT OF STREAM WITH DISK

The case of the impact of the stream with a circumstellar disk is especially interesting. According to the scenario developed in Paper I, the disk edge travels nearly in a simple periodic orbit with average radius ϖ_d. The vertical structure of the preimpact disk edge should be nearly hydrostatic. If the temperature of the preimpact stream is comparable to that of the preimpact disk edge, Table 1 and Figure 1 show that the Gaussian thickness of the stream exceeds the Gaussian thickness of the disk edge by factors typically of 3 or 4. Hence, even if in the orbital plane the density of the disk edge is several orders of magnitude larger than the density of the stream, the disk density will be considerably smaller at 1 or 2 scale heights of the stream above and below the midplane. At these distances, the material behind the bow shock must be carried by the stream's inward motion over the top and bottom of the disk in a manner similar to supersonic flow past blunt obstacles (see Fig. 2).

This possibility was foreseen in Paper I (p. 398), and we conjectured there that the large slip velocities present in the interface would lead to a highly turbulent wake whose largest eddies have sizes comparable to the disk thickness. Eventually, however, all of the material in the stream will still be entrained in the disk by the fundamental tendency of the gas to fall toward the orbital plane.

IV. OBSERVATIONAL IMPLICATIONS

A "hot spot" model invoking stream-disk impacts seems to account for several of the observed features in the light curves of cataclysmic variables during their quiescent stages (Smak 1971; Warner and Nather 1971; Krzeminski and Smak 1971). In particular, the "flickering" characteristic of the light curves of these systems has now definitively been associated with the activity of the hot spot, and we (Shu 1975) have suggested that the power spectra of the observed time variations (see, e.g., Robinson 1973, Fig. 6) are indicative of the turbulence induced by the unstable nature of the postimpact flow.

Until now, however, it has not really been understood why the flickering should be observed at all orbital phases excluding eclipses by the contact component. The disk is believed to be fairly massive ($\sim 10^{-5}$ $M_\odot$, Smak 1972; Warner 1973), and it should be opaque to optical radiation. Thus, if the shock front produced by the stream-disk impact were confined only to the front face of the disk edge, the hot spot would be unobservable for a wide range of orbital phase around 0.4 P in eclipsing systems. This deduction fails to correspond to the observed nature of the flickering activity, and we conclude that a better correspondence

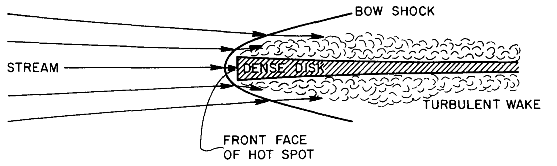

FIG. 2.—Schematic diagram of stream-disk impact. The equatorial plane is viewed edge-on. A bow shock partially arrests the inward motion of the stream, forcing the streamline in the midplane to turn parallel to the disk edge (out of the plane of the paper; see Fig. 1). Material at large heights sweep over and under the disk, leaving a turbulent wake.

would be obtained if the hot spot had a three-dimensional structure more in accordance with Figure 2.

Further support for this type of model is provided by observations of the X-ray binary in Hercules. Various workers (Pines *et al.* 1973; Middleditch 1976) have already proposed that the X-ray absorption dips seen periodically in Her X-1 (Giacconi *et al.* 1973; see also Boynton *et al.* 1973) are associated with the presence of material above the orbital plane at heights substantially greater than the normal thickness of the disk. Assuming $\dot{M} \sim 3 \times 10^{-9}\ M_\odot\ \mathrm{yr}^{-1}$, $\epsilon \sim 0.03$, $P =$ 1.7 d, $d = 6 \times 10^{11}$ cm, and $M_D/M_C = 0.6$, we easily estimate from our tables that a roughly correct column density of material, $\sim 10^{23}\ \mathrm{cm}^{-2}$, would be naturally provided by the high-latitude portions of the stream.

We shall not speculate here on the cause of the marching of the dips in orbital phase with changing 35^d X-ray cycle; however, we do conjecture that the reprocessing of some of the X-rays in the turbulent wake is responsible for the main part of the optical flickering reported by Moffett, Nather, and Vanden Bout (1974). In this regard, we note that the total impact luminosity of the hot spot, $\sim 2 \times 10^{32}$ ergs s^{-1}, in the Hercules system is a factor of 6 too small to account for the magnitude of the flickering which is observed.

We thank Lawrence Anderson, John Middleditch, and Steve Weber for useful conversations. We are grateful to Kinsey Anderson for financial support of the graduate studies of S. H. L. through NASA grant NGL 05-003-497 to the Space Sciences Laboratory at Berkeley. The numerical calculations for this paper were performed at the Berkeley Computing Center.

REFERENCES

Boynton, P. E., Caterna, R., Crosa, L., Deeter, J., and Gerend, D. 1973, *Ap. J.*, **186**, 617.
Flannery, B. P. 1975, *Ap. J.*, **201**, 661.
Giacconi, R., Gursky, H., Kellog, E., Levinson, R., Schreier, E., and Tananbaum, H. 1973, *Ap. J.*, **184**, 227.
Krzeminski, W. and Smak, J. 1971, *Acta Astr.*, **21**, 133.
Lubow, S. H., and Shu, F. H. 1975, *Ap. J.*, **198**, 383.
Middleditch, J. 1976, Ph.D. thesis, Univ. of Calif., Berkeley.
Moffett, T. J., Nather, R. E., and Vanden Bout, P. A. 1974, *Ap. J.* (*Letters*), **190**, L63.
Pines, D., Pethick, C. J., and Lamb, F. K. 1973, in *Sixth Texas Symposium on Relativistic Astrophysics*, ed. D. J. Hegyi (*Ann. N. Y. Acad. Sci.*, **224**, 237).
Prendergast, K. H., and Tamm, R. E. 1974, *Ap. J.*, **189**, 125.
Robinson, E. L. 1973, *Ap. J.*, **180**, 121.
Shu, F. H. 1975, in *IAU Symposium No. 73*, ed. S. Mitton and J. Whelan, in press.
Smak, J. 1971, *Acta Astr.*, **21**, 15.
———. 1972, *ibid.*, **22**, 1.
Warner, B. 1974, *M.N.R.A.S.*, **168**, 235.
Warner, B., and Nather, R. E. 1971, *M.N.R.A.S.*, **152**, 219.

STEPHEN H. LUBOW and FRANK H. SHU: Berkeley Astronomy Department, Leuschner Observatory, University of California, Berkeley, CA 94720